Workspace Shape and Characteristics for Human Two- and Three-Fingered Precision Manipulation

Ian M. Bullock*, *Student Member, IEEE*, Thomas Feix, *Member, IEEE*, and Aaron M. Dollar, *Senior Member, IEEE*

***Abstract*—*Goal:* To study precision manipulation, which involves repositioning an object in the fingertips and is used in everyday tasks such as writing and key insertion, and also for domain-specific tasks such as small scalpel cuts, using tweezers, and hand soldering. *Methods:* In this study, the range of positions (workspace) through which 19 participants manipulated a 3.3–4.1 cm-diameter object are measured with a magnetic tracker. Each participant performed two conditions: a two-finger thumb-index finger condition and a three-finger thumb-index-middle finger condition. *Results:* The observed workspaces, normalized to a 17.5 cm hand length, are small compared to free-finger trajectories; for the two-finger trials, 68% of points are within 1.05 cm of the centroid and 95% are within 2.31 cm, while the three-finger case shows a narrower distribution, with 68% of points within 0.94 cm of the centroid and 95% of points within 2.19 cm. The longest axis is a long thin arc in the proximal-palmar plane. Analysis of fingertip workspaces shows that the index fingertip workspace volume is the most linear predictor of object workspace ($R^2 = 0.98$). *Conclusion:* Precision manipulation workspace size and shape is shown, along with how the fingers are used during the manipulation. *Significance:* The results have many applications, including normative data for rehabilitation, guidelines for ergonomic device design, and benchmarking prosthetic and robotic hands.**

***Index Terms*—Dexterous manipulation, ergonomics, haptic interfaces, human hands, robot hands.**

I. Introduction

CONSIDERING the immense scope and broad reaches of the topic, there has been relatively little work done related to understanding normal human hand use, and especially quantifying function. More prior research has studied human grasping [1]–[4] and finger force modulation [5], while understanding the human hand's kinematic capabilities during dexterous, within-hand manipulation [6] has been largely ignored. Some studies have analyzed the kinematic capabilities of individual fingers in healthy participants [7], [8], as well as comparing the finger capabilities of participants with impaired hand functionality [9]–[11]. However, only a few studies (see Section II) directly consider the precision manipulation task of multiple fingertips interacting with an object, as in the present work.

Precision manipulation, which is the hallmark of humankind's superior dexterity, is key to the ability to perform a large number of daily tasks. Precision manipulation is used in tasks such as writing or using a haptic input device (see, e.g., [12] and [13]). Knowledge of the precision manipulation workspace can be applied to the analysis of surgical technique and dexterity [14], or to improve the design and usage of hand-held medical devices [15], including teleoperated surgical robots [12]. Devices and methods can be tailored to take advantage of the most natural motion ranges, potentially resulting in greater precision, lower strain, and less energy consumption than larger wrist and whole-arm motions. For example, if only within-hand movement is needed, the upper limb can be braced to increase precision and reduce fatigue [16]. This kinematic information can also be used to better target rehabilitation efforts [17] or surgery of an impaired hand [18], and to benchmark prosthetic or robotic hands [19]–[21].

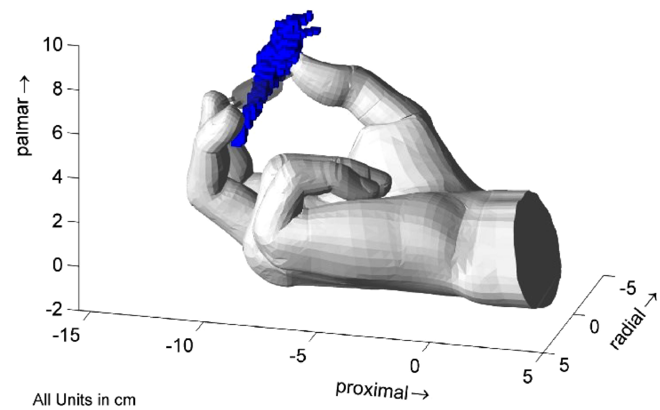

Fig. 1. Three-fingered precision manipulation workspace example. A voxel grid is fitted to the original workspace points, both to calculate workspace volume and for visualization.

The current work seeks to experimentally determine the *precision manipulation workspace* of the human hand and builds on an initial conference paper by the authors [22]. We define this workspace as the range of motions through which a person can feasibly move an object held between the fingertips, without removing or replacing the contact, or allowing the object contact point to slide [6]. Fig. 1 shows a sample workspace from one subject, indicating the approximate size, shape, position, and orientation of the workspace for the tested object size and three-finger contact condition. We also examine the tradeoffs in manipulation workspace between using two and three fingers. While using three or more fingers may give additional stability, we hypothesized that, due to additional constraints, the precision manipulation workspace where only the thumb and index finger are used would be larger than when the middle finger is also involved.

Manuscript received October 17, 2014; revised February 6, 2015; accepted March 18, 2015. Date of publication March 31, 2015; date of current version August 18, 2015. This work was supported in part by the Gustavus and Louise Pfeiffer Foundation and the National Science Foundation under Grant IIS-0953856. *Asterisk indicates corresponding author.*

*I. M. Bullock is with Yale University, New Haven, CT 06511 USA (e-mail: bullock.ian@gmail.com).

T. Feix and A. M. Dollar are with Yale University.

Color versions of one or more of the figures in this paper are available online at http://ieeexplore.ieee.org.

Digital Object Identifier 10.1109/TBME.2015.2418197

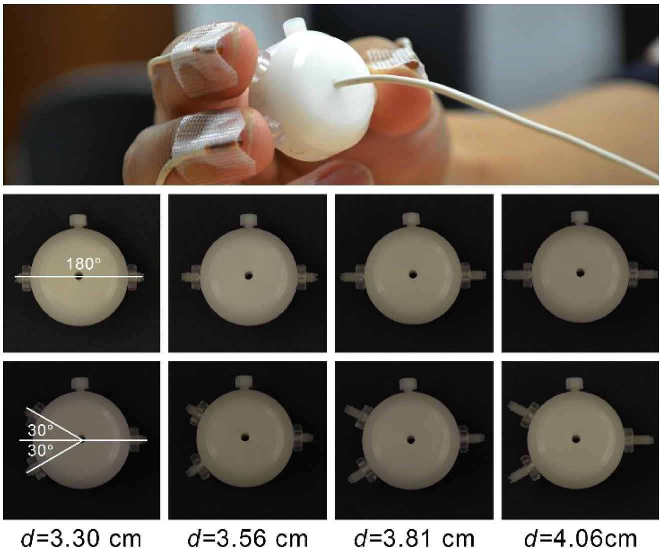

Fig. 2. Four sizes of the pointed object used for manipulation. The object is scaled to one of the four discrete sizes based on participant hand length. The set screw points help to maintain a fixed contact location throughout the manipulation trials.

The remainder of this paper is structured as follows. The next section provides an overview of related work, particularly hand workspace estimation. Section III describes the study methodology used. Section IV shows various characteristics of the manipulation workspace across all participants, as well as the patterns of finger usage during manipulation. Section V analyzes the workspaces and trends and discusses broader applications. Finally, Section VI discusses limitations of the study and potential future work.

II. Background

Our current work differs from existing work by directly studying the within-hand kinematic workspace of human precision manipulation of a real nonzero size object. Some existing work which has looked at related tasks will be discussed.

Kuo *et al.* [23] examined *functional workspace* of 20 participants by calculating the area of intersection of the free thumb and finger trajectories, to estimate the ability of the hand to move a small object within a precision pinch grasp. The work illustrates the resulting 3-D workspaces and analyzes relationships between finger length and the workspace for each thumb–finger combination. A follow-on work does some additional fitting of the resulting shapes [24]. However, the current work differs by analyzing manipulation workspace of a real nonzero size object directly and considers workspace as a 3-D volume rather than the simplified 3-D surface used in [23]. It is also important to note that the interaction with the object creates a different kinematic structure from the free swing trajectories of the fingers.

Youm and Chung [25] modeled a workspace using a technique similar to the Kuo *et al.* [23] workspace intersection method. However, this work models only a planar workspace, assuming that manipulation in a three-fingered grasp is always along the medial plane of the hand. The present work does not make this simplifying assumption and considers experimental data for the full 3-D workspace.

The manipulability of the thumb and index finger pinch in three postures is analyzed in [26]. The results indicate, for example, that the index finger posture plays a greater role in determining manipulability than the thumb posture. This work differs because it considers only three poses with a small stick object and focuses on manipulability, rather than the current work's larger object and continuous kinematic view.

Some work in the robotic domain has looked at precision manipulation workspace. For example, Borras and Dollar [27] looks at the workspace of a three-fingered symmetric robotic hand using a framework inspired from the parallel platform literature. Odhner and Dollar [28] analyzed planar workspace of a symmetric, underactuated two-finger hand. Ma and Dollar [29] applies a linkage-based analysis to the workspace of a similar hand. Finally, Cui and Dai [30] analyzes how a flexible palm influences the workspace and manipulability of the three-fingered metamorphic hand. The present work differs from previous robotic efforts in that it looks at the specific case of the human hand, taking an experimental approach to assessing the workspace.

Some works have looked at related tasks, but from a force perspective rather than a kinematic perspective. Rácz *et al.* [31] looked at the force coordination patterns of the thumb, index, and middle fingers while performing simple tasks with a three-load cell object. Their results indicate a strong synchrony of normal force modulation by each finger during the tasks tested. However, this work did not involve significant displacement of the overall object. Many motor control related works do study finger forces in detail; see [5] for a review. However, these works generally consider forces and overall hand and arm movements, rather than the kinematics and within-hand behavior that are the focus of the present work.

Finally, Gilster *et al.* [32] looked at the finger contact points used during grasping and lifting of a cylinder and other objects. This study indicates comfortable grasp point positions for a three-fingered cylinder grasp are to have the index and middle finger positions at approximately $\pm 20 - 30^{\circ}$ relative to a position opposite the thumb. These results were utilized in this work to determine the grasp point (angles of $\pm 30^{\circ}$, see Fig. 2) on the pointed object used in this study.

III. Materials and Methods

Our experimental protocol involves unimpaired human subjects manipulating a pointed object (see Fig. 2) held between the thumb and forefinger or thumb, forefinger, and middle finger, while the relative position of the center of the object with respect to a hand base coordinate frame is measured. A pointed object was used to minimize changes in finger contact location, while still allowing free pivoting of the object. Magnetic tracker sensors (see Fig. 3) and visual feedback (see Fig. 4) were used.

A. Participants

Nineteen participants completed the experiment. They are aged 18–31 (median 25), with six male and 13 female

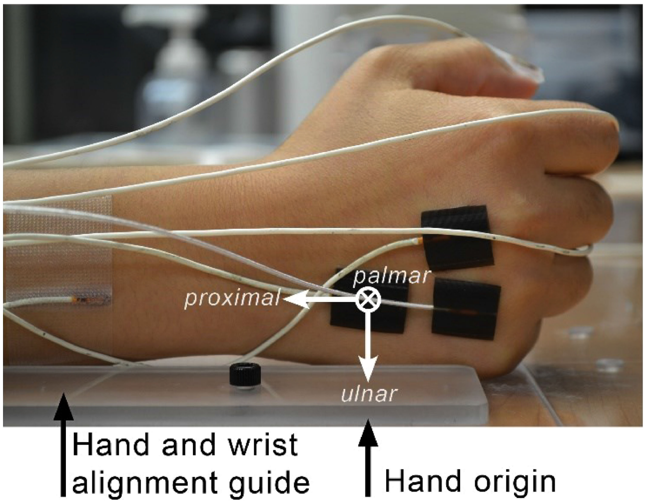

Fig. 3. Hand coordinate frame. The sensor defining the origin is placed one-third of the way from the continuation of the wrist flexion crease to the bump from the fourth metacarpal head, along the fourth metacarpal. All motions are referenced relative to this sensor.

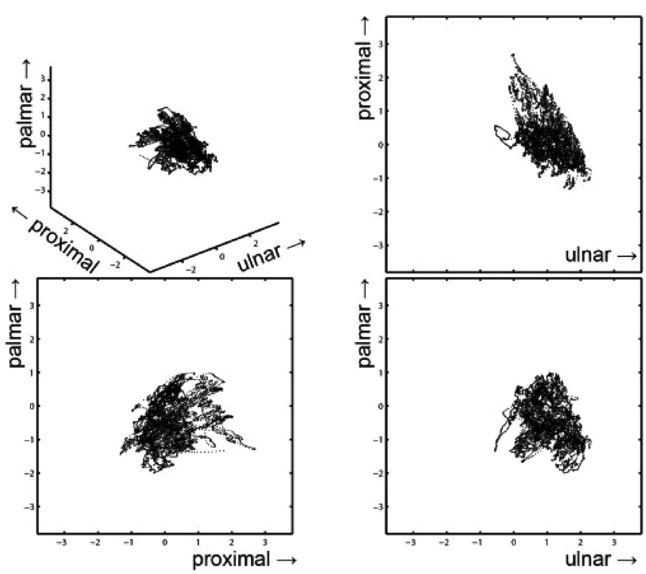

Fig. 4. Visual feedback. The four views shown were displayed on a monitor in front of the participant. Axes and axis labels were not shown during the actual experimental trials to reduce distractions, but the plot locations are the same in this figure as were used on the monitor during the experimental trials. Participants were instructed both to trace out as much area on the screen as possible, and also to fill in the area.

participants. Participants were recruited from the local university community. Hand length (wrist crease to middle fingertip) ranged from 15.5 to 19.8 cm, with a median hand length of 17.5 cm. The measurement setup required that all subjects be right handed and have normal unimpaired hand function. Specifically, any participants with history of significant hand and wrist injury were excluded from participation. The study was approved by the local IRB and all subjects were individually consented and financially compensated for their participation.

B. Equipment

A trakSTAR magnetic tracking system (Ascension Technologies, Burlington, VT) with a medium range transmitter and eight MODEL 180 2 mm diameter sensors were used. Each sensor provides 6-DOF data (x, y, and z position, and three rotations) at the configured, recommended sampling rate of 80 Hz. The positional accuracy of the system is 1.4 mm RMS and the angular accuracy is 0.5° RMS. The three trakSTAR sensors to be placed on the back of the hand were inserted into small rubber sleeves (see Fig. 3) to reduce unintended rotation around the long axis of the sensor during the experiment. The object sensor was fixed in the center of the object using a nylon screw.

The object shown in Fig. 2, referred to from here on as the "pointed object," was machined to allow three adjustable 4–40 (2.6 mm diameter) nylon setscrew finger contact points at 30 degree angle increments. The final object has a mass of 11 g, excluding the magnetic sensor. These were set to provide 3.30, 3.56, 3.81, or 4.06 cm effective diameter, depending on participant hand length. This range was picked based on anthropometric data [33] to allow object scaling from a 1% female hand to a 99% male hand, as well as informal tests that showed this to be a comfortable object size that ought to give a large workspace.

Visual feedback was provided on a 27 in LCD monitor 1 m in front of the experimental table to help participants thoroughly explore their position workspace; a diagram of the views used can be seen in Fig. 4. Three views were aligned with two anatomical axes of the hand (distal-proximal, radial-ulnar, dorsal-palmar), while the fourth view was a perspective view. During each trial, participants were instructed to visually trace out as large a workspace volume as possible, and to fill in this volume as best they can. A goal-based variant of this visual-feedback exploration approach was considered, but ultimately decided against due to the added risk of biasing the results based on the goal characteristics, rather than capturing a more natural range of movement.

C. Procedure

Some preparation was performed before the experiment. First, the participants removed any metal-containing objects, such as keys and cell phones, from their pockets, since metal could distort the magnetic fields emitted by the magnetic tracking system. Then, the participants were shown a short series of slides explaining the experimental procedure in detail. Participants were instructed to minimize any sliding of the pointed object at the pointed contact points, and to make sure that the initial contact points were within the area of the distal half of each finger pad used. Participants were also instructed to avoid removing any fingers from the object during a trial. In this manner, the participant is prevented from using sliding or finger gaiting during the trials. Although this constraint was participant enforced, the experimenter did also observe the participants to make sure they had understood the instructions and were not violating the constraints.

Sensors were then attached to the subject, as can be seen in Fig. 2. 3M Transpore tape was used to attach four sensors to the fingernails and wrist. Three more sensors were inserted into

$1.5 \times 1.5 \times 0.3$ cm rubber mounts and attached to the back of the hand using Top Stick Men's Grooming Tape. The sensor cords were draped over the participant's shoulders, and a hook and loop strap was wrapped around the sensors and participant's forearm to provide effective strain relief to prevent the cables from disturbing the sensor positioning. The participant was instructed to flex their fingers fully while setting the sensor cable rest lengths to avoid any tugging of the sensors during the study. Hand length and width were measured according to [33]. Specifically, the length measurement is taken from the wrist flexion crease to the tip of the middle finger. The object size to be used was calculated according to the equation $d = 0.2\, l_h$, where d is the object diameter and l_h is the hand length, both in centimeters. The diameter closest to one of the four discrete target diameters was then set. The final sensor was placed inside the object and held in place with a nylon set screw.

The hand position for the trials can be seen in Fig. 3. A plastic alignment guide was used to help the participant keep their wrist approximately straight and their hand in the same location for each trial, while avoiding the constraints on hand motion that other bracing methods could impose. Subjects were instructed to keep their arm and the back of their hand aligned along this guide during the experiment in order to reduce hand base frame movements due to skin motion. The alignment guide and chosen hand position could have a minor impact on the motions observed. The table provides a planar constraint under the hand, which was not observed to provide a limitation on the participant's motion, but theoretically could restrict certain motion trajectories in the ulnar direction. Hand orientation affects the relative orientation of the gravity vector, which could make it easier to perform certain motions without dropping the object. However, this should only affect the very edges of the workspace where manipulation becomes difficult.

For this work, two blocks of trials involving a pointed object (see Fig. 2) manipulated with two and three fingers will be considered. The full study did include additional trials with a spherical object and individual finger movements. These trials were used to evaluate finger surface usage and are discussed separately in [34]. These additional trials are noted here simply to give a full understanding of the set of tasks each participant had to perform during their experimental session. The order of the trial blocks was randomized. Before each block of three trials, a 1 min practice period was given for the participant to explore the workspace without visual feedback. Following the practice, three 2 min workspace trials were performed. After every trial, a rest period of about 30 s was given. In total, the duration of the trials was about 80 min, including the time required for the experimenter to switch between trial conditions.

D. Workspace Volume Calculation

A voxel binning method was used to calculate the workspace volume, similar to that used in [19]. Specifically, workspace points from each trial were binned into a 3-D grid of voxels. The grid spacing, or size of each bin, was set using a 95% confidence interval for the deviation of the hand reference frame sensor points, which is 2.15 mm. This number sets a reasonable range within which workspace points cannot be effectively discriminated. The effect of bin size on resulting workspace volume was evaluated, and it was determined that volume increases roughly linearly with increasing voxel size. This linear scaling makes the ratio of the workspaces more meaningful than the absolute size values. It was also confirmed qualitatively that 2.15 mm is a large enough voxel edge width to prevent frequent holes in the workspace volumes due to sparse data points. The final volume is calculated as the sum of the individual voxel volumes that contain at least one data point.

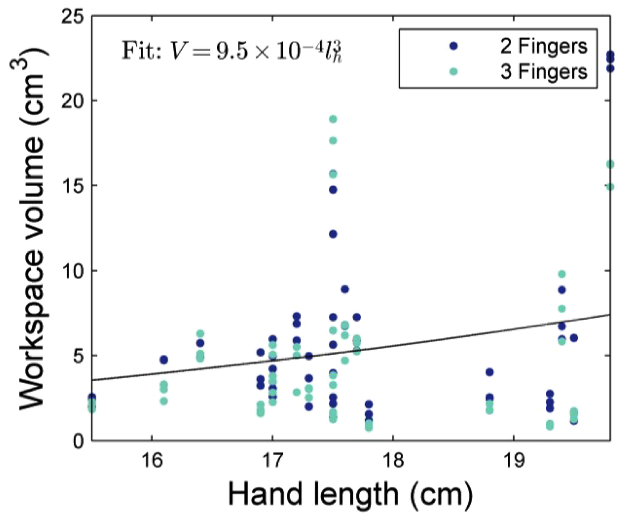

Fig. 5. Workspace volume as a function of hand length. A slight increase in volume is observed as hand length increases, but a great deal of variability occurs which is not explained by hand length alone.

E. Normalization and Trial Combination

Unless otherwise stated, all data is normalized to the median 17.5 cm hand length from the study participants. Specifically, the workspace points for a given participant i are scaled by

$$(x', y', z') = \left(\frac{\bar{l}}{l_{hi}}x, \frac{\bar{l}}{l_{hi}}y, \frac{\bar{l}}{l_{hi}}z\right) \tag{1}$$

where $\bar{l}$ is the median hand length, l_{hi} is the given participant's hand length, and the primed coordinate frame is scaled relative to the raw data in the unprimed frame. The desired effect is to view all data as if it came from a participant with median 17.5 cm hand length, while keeping the data in units that are easier to understand intuitively.

With the exception of some initial statistical tests and the analysis for Fig. 5, the three trials for each participant and experimental condition were simply combined together into one larger trial for the analysis in this work.

F. Statistical Methods

A few statistical methods are used frequently to analyze the results. For positions in $\mathcal{R}^3$, confidence intervals are often given for the individual (x, y, z) coordinates by simply calculating a 95% confidence interval based on the standard error for each

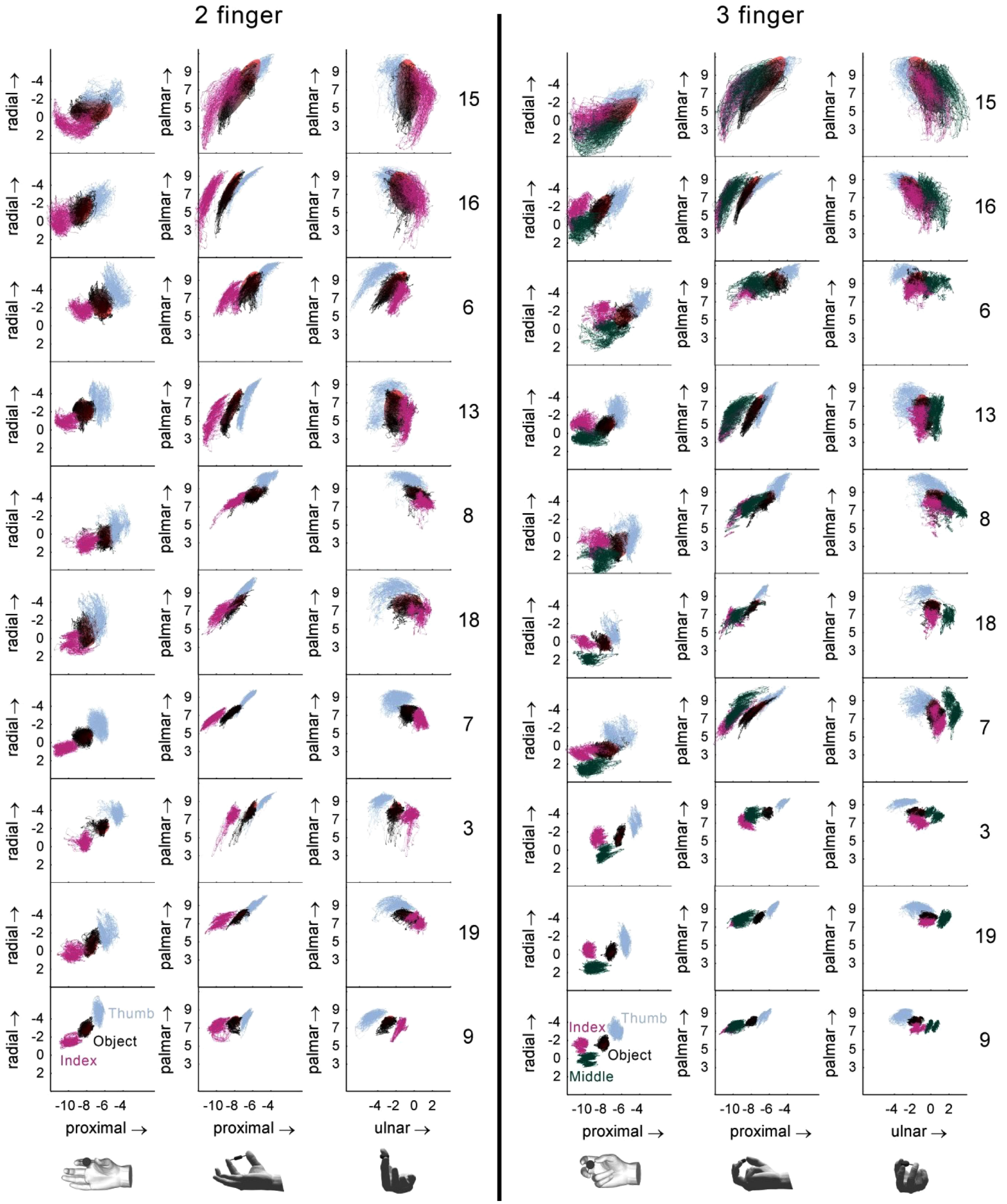

Fig. 6. Two- and three-finger object and finger workspaces for ten participants. All units are cm. The colors used are explained in the lower left corner of the two- and three-finger sections. Each row corresponds to a particular participant (as indicated by the participant number on the right), while each column corresponds to a particular workspace view. The left set of three columns is for the two-finger case, while the right set of three columns is for the three-finger case. The participants are sorted in descending order from top to bottom by the sum of their two- and three-fingered workspaces. Every other participant is shown due to space considerations. Ellipsoids are fitted to the object workspace using PCA and the variance along each of the PCA axes.

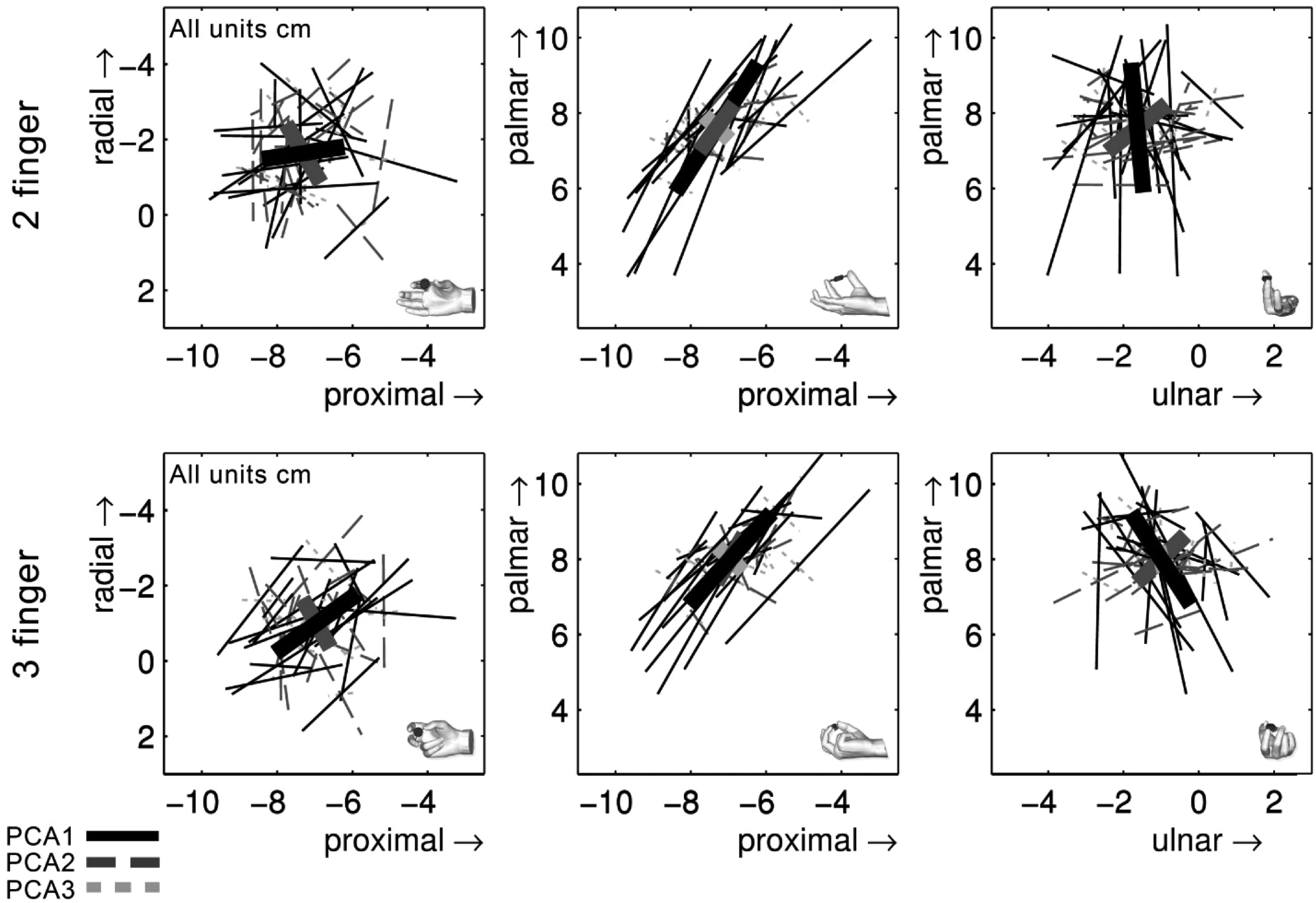

Fig. 7. Principal components for all participants. PCA is used to find an orientation for three principal vectors for each participant's workspace. The length of these vectors is then set by extending the axes 1.96σ in either direction. The first axis is darkest and the third axis lightest. Different dash patterns are also used for the non-summary axes. These vectors are used to define the axes of the ellipsoids in Fig. 6. Finally, an average of all the participants' PCA vectors is taken and plotted as a thicker set of lines.

individual variable. To assess the variability of a set of orientations (often expressed as unit vectors in $\mathcal{R}^3$), we expand a cone centered around the mean orientation until it contains a given percentage (e.g., 68%) of the orientation data. The resulting semivertical angle for the cone gives an intuitively understandable measure for how spread out the orientation data is. This method is also discussed in [34]. Some conventional methods which apply only to certain aspects of the data are discussed when relevant in the context of the results.

IV. Results

Several statistical tests were performed initially to check for any complicating effects in the dataset. These initial tests are performed without the normalization discussed in Section III-E. By fitting a linear regression model to the cube of hand length, and testing for significance of the slope term, it was found that hand length significantly affects the resulting workspace ($p = 0.001$) (see Fig. 5). The effect of sex on volume was tested by performing a t-test for the means of all female and male workspace volumes in the study, which gave an almost significant $p = 0.07$, but if the effect of hand length on volume is taken into account by subtracting out a compensating term based on the equation in Fig. 5, this difference in means is reduced and is no longer significant ($p = 0.49$). It was initially hypothesized that workspace volume would increase with participant experience. This was tested by performing a linear regression for the relationship between volume and trial number, but this did not give a statistically significant slope parameter ($p = 0.6$). On average, the workspace volume increased a modest 24% from the first to third trial of each block, but again the slope parameter for the corresponding linear regression is not statistically significant ($p = 0.3$). After accounting for hand length effects by subtracting a compensating term based on the equation in Fig. 5, a linear regression of volume versus object diameter does not yield a statistically significant slope term ($p = 0.8$) for the range of sizes utilized in this study. Following this initial analysis, sex and any trial order effects were not considered in the following.

The relationship between workspace volume and hand length is shown in Fig. 5. It is hypothesized that volume should scale as the cube of hand length. This hypothesis should hold if the human hand scales in a manner which preserves relative link lengths and maintains constant joint limits, in which case the conversion between workspace volumes could be thought of

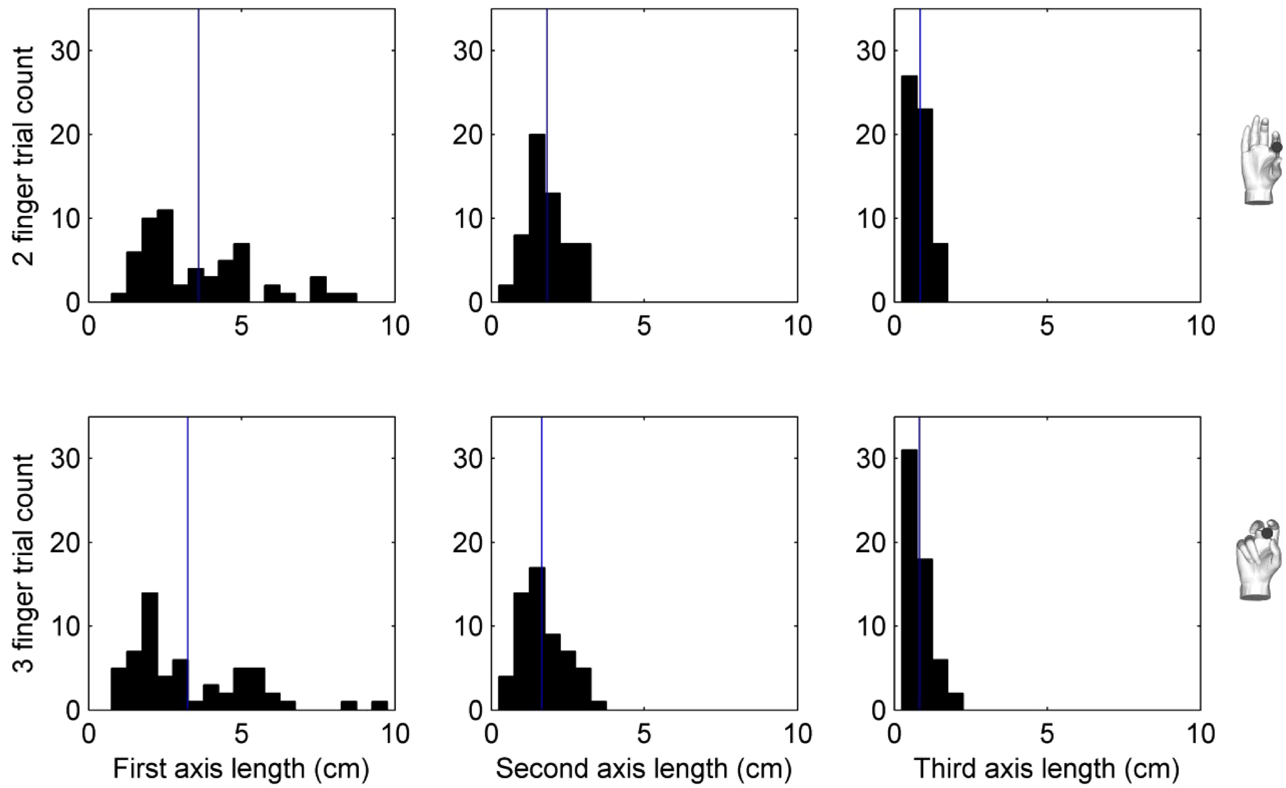

Fig. 8. PCA axis length distributions. Histograms are shown for the first, second, and third PCA axis length in the two- and three-finger cases. Lengths are calculated by the variance of the workspace data along that particular axis; the axes are shown graphically in Fig. 7. The vertical lines indicate means.

as a simple unit conversion between link lengths (given that object size has been scaled deliberately with hand length in this study). With this hypothesized cubic model, the fitted equation obtained to calculate expected volume for a given hand length is $V = 9.54 \times 10^{-4}\, l_h^3$, where V is the volume in cubic centimeters and l_h is the hand length in centimeters. The increase in volume with hand length is statistically significant, with $p = 0.001$. While the increase in volume with hand length is significant, it should be noted that this statistical test does not confirm whether the simple cubic model proposed is the best model.

Combined overlaid three-trial workspaces for ten out of 19 participants are shown in Fig. 6 for both the two- and three-fingered conditions, along with individual finger workspaces. The participants were sorted by workspace volume, and then, every other participant was plotted, resulting in the ten participants shown. All data have been normalized to the 17.5 cm median hand length from this study as discussed in Section III-E. Ellipsoids are shown in red over the black object workspace points and are defined by three axes from principal component analysis (PCA), i.e., the eigenvectors of the covariance matrix. The length of the axes is defined by a $\pm 1.96\,\sigma$ range for the data, projected onto each axis, and the center location is the mean of the data. The ellipsoid is a simplified way to visualize the work space, while preserving key characteristics of the workspace, such as position, orientation, and size. This figure demonstrates the characteristics of participant variability—many participants have smaller, more spherical shaped workspaces, while the larger volume workspaces usually show an elongated shape with a characteristic arc in the proximal-palmar plane. The participants with the two largest workspace volumes appear able to extend this proximal-palmar plane arc to greater thickness.

Fig. 6 also shows the workspace of the individual fingertips during manipulation for all participants, as well as the differences between finger usage in the two- and three-finger cases. The workspace of the index fingertip in the two-finger case actually seems to be quite similar to the workspace of the middle fingertip in the three-finger case. In the three-finger case, it seems that the motions of the index and middle fingers generally trace out similar, but offset, trajectories. This is especially evident by the almost complete overlap of the index and middle finger point clouds in the proximal-palmar plot.

On average, the two-fingered workspace is 38% larger than the three-fingered workspace, with a paired t-test giving $p < 0.001$. However, it is difficult to see clear differences in workspace shape between the two- and three-finger cases. One noticeable difference is that for the lowest volume participants, the three-fingered workspaces seem noticeably more contracted than in the two-fingered trials, with fewer outlier points.

The principal axes for each participant's object workspace are shown in a combined view in Fig. 7. An overall average of the axes is taken and plotted as a thicker set of axes in the same color scheme. Specifically, the summary axis directions are computed by taking a simple average of the vectors in Euclidean space [35], after projecting the vectors into a single hemisphere to avoid any issues with averaging equivalent "negative" and "positive" versions of the same vector. The directions are first

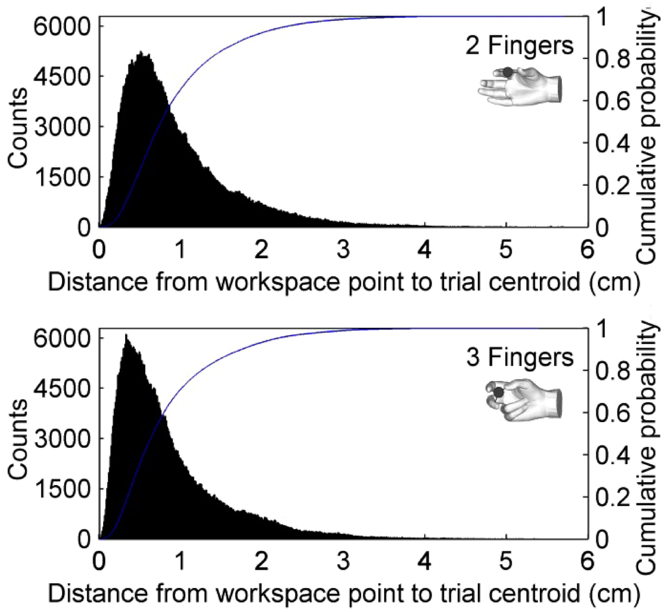

Fig. 9. Distribution of distances from trial centroid. These two plots show the probability of a given trial point being found a certain distance away from the trial centroid in both the two and three-fingered cases. The distributions are similar, with the three-fingered distribution dropping off slightly more sharply.

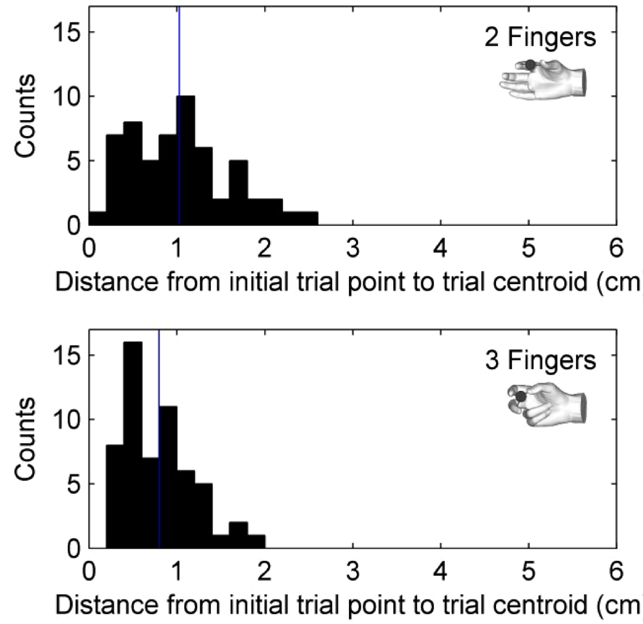

Fig. 10. Distribution of distance from initial trial starting points to trial centroids. The means are indicated by the vertical lines in each of the two plots. For the two-fingered case, the mean start distance from the trial centroid is 1.0 $\pm$ 0.1 cm, while it is 0.8 $\pm$ 0.1 cm for the three-fingered case (both normalized distances for a 17.5 cm hand).

normalized, so that each participant's data are weighted equally. The mean location and axis lengths are a simple average of the mean location and lengths for the individual participants.

Overall, the principal axes shown in Fig. 7 appear similar between the two- and three-fingered conditions. The primary axis orientation is particularly similar between the two conditions in the proximal-palmar plane. However, there is more of an overall shift in orientation when viewed in the proximal-radial plane (left plots), or in the palmar-ulnar plane (right plots). Specifically, in the two-finger trials, the axis aligns closely to the proximal and palmar axes, while in the three-finger trials, it tilts more in the direction of the added middle finger.

The distribution of principal axis lengths can be seen in Fig. 8. These distributions help illustrate what proportion of participants can achieve a given workspace size along the principal axes found. The first axis shows a bimodal or multimodal distribution with a few extreme outliers (especially in the three-finger trials. The second axis length appears to be much closer to a normal distribution. The third axis length is, on average, only half the length of the second axis. Specifically, the first, second, and third average axis lengths are (2.0, 1.1, 0.5) cm, respectively, for the two-finger case and (1.8, 1.0, 0.5) cm for the three-finger case. One should note that the lengths (as defined from the covariance matrix) will always progressively decrease due to the nature of PCA, but the extent of this decrease can still be meaningful. In addition to breaking down the results by the principal axis vectors, the workspace data can also be analyzed more simply relative to the mean location.

Fig. 9 shows the distribution of the data's distance from the centroid of the trial it was taken from. The centroid for a trial is simply the arithmetic mean position of all the object points for that trial, corresponding intuitively also to the center of mass of the trial points, considering each trial point to be a point mass of equal mass. This figure shows data from every trial for all 19 participants, broken up by the two- and three-finger manipulation cases, with 547 200 total points sampled at 80 Hz. The numerically determined cumulative distribution function (cdf) is plotted as a curve on each plot and shows the ratio of points within a distance $0 < d < x$ from the centroid, where x is the maximum distance being evaluated. For the two-fingered case, the cdf shows that 68% of points are within 1.05 cm, 95% of points are within 2.31 cm, and 99% of points are within 3.36 cm. For the three-fingered case, the distribution of points is slightly closer to the centroid; the cdf shows that 68% of points are within 0.94 cm, 95% of points are within 2.19 cm, and 99% of points are within 3.16 cm.

During the study, the participants were instructed to position the object within their fingertips in a comfortable, neutral resting position at the start of each trial. We hypothesized that this relaxed start position should be close to the center of the observed position workspace. The distances from the initial object position of each trial to the centroid for that trial are shown in Fig. 10. The results indicate the two-fingered and three-fingered mean distances from the initial trial position to the trial centroid are 1.0 ± 0.1 and 0.8 ± 0.1 cm, respectively (using a standard error based 95% confidence interval). By looking at the distribution of distances of points from the centroid, the percentile for these initial point distances can be calculated. The two- and three-finger percentiles for the start location distance to the centroid are $57 \pm 7\%$ and $51 \pm 7\%$, respectively. This indicates that for the two-finger case, 57% of the data points are closer to

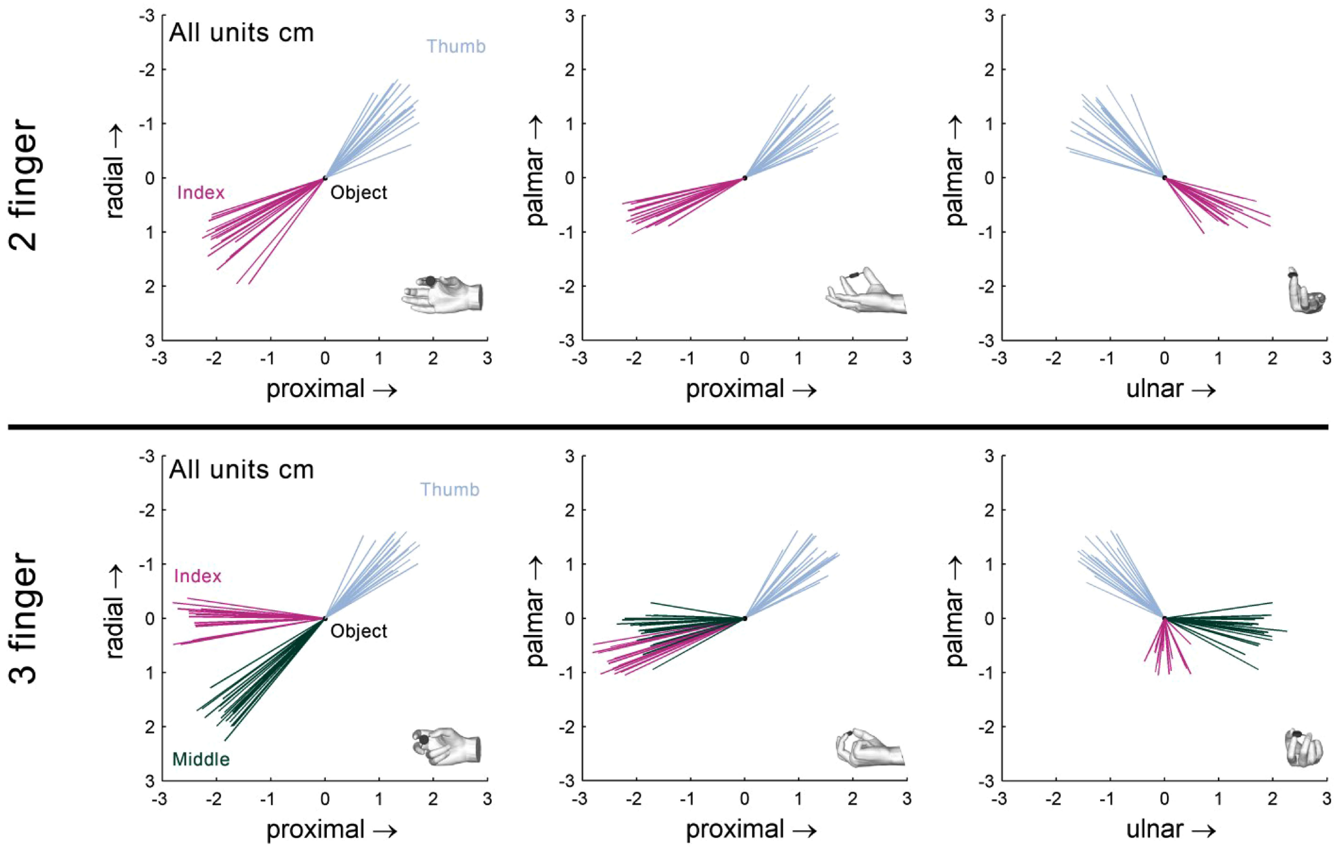

Fig. 11. Average finger positions relative to average object positions. View planes are the same as in Fig. 7. For each participant and set of three trials, centroids (averages) are calculated for the finger and object workspaces. The finger positions are then plotted by their position relative to the object. These plots show what angles the fingers are generally used at during the two- and three-fingered manipulation trials.

the centroid than the initial point, whereas for the three-finger case, it is 51%. The difference between these two percentiles is insignificant ($p = 0.12$). Thus, our original hypothesis that the initial position for each trial should be particularly close to the trial centroid is contradicted—the start locations are merely at an average distance from the trial centroid, though still within 1 cm.

Fig. 11 shows the centroid (average) of each fingertip workspace relative to the object positions and demonstrates that across all participants, these angles are quite consistent. Specifically, the semivertical angles of cones containing 68% of the orientations are all within the range of 8–13°, as seen in Table I. In general, the thumb is used for precision manipulation in a position, which is significantly further in the palmar direction than the fingers are. The index finger in the two-finger case generally appears to be in a position roughly centered between where the index and middle finger positions are in the three-finger case. The average object to finger vectors can be seen in Table I.

Fig. 12 shows the correlation of the individual finger workspace volumes to the object workspace in the two- and three-finger cases. For the two-finger case, R^2 values for the thumb and index finger are 0.75 and 0.94, respectively. The slopes, with ± standard error, are 0.95 ± 0.06 and 0.98 ± 0.03 for the thumb and index finger, respectively. R^2 values for the three-finger case for the thumb, index, and middle fingers are 0.79, 0.98, and 0.96, respectively. The slopes for the thumb, index, and middle fingers are 0.97 ± 0.07, 0.91 ± 0.02, and 0.74 ± 0.02, respectively, where the standard error follows the "±." Overall, the volume of the thumb and index workspaces scale very similarly to the workspace of the object, while the middle finger traces out a larger workspace volume than the object does. The index finger workspace to object workspace scaling has the best R^2 value, whereas the thumb workspaces do not fit a linear trend as well, especially in the two-finger trials.

V. Discussion

The results show the precision manipulation workspaces and fingertip usage of all 19 participants. First, the workspace characteristics will be discussed in terms of size, shape, center location, and inter-participant variability. Then, the workspace differences observed between the two- and three-finger conditions will be analyzed. Finally, applications will be discussed.

A. Workspace Volume

Overall, the workspace volume achieved is small, much smaller than the volume the fingertip can fill in free motion. The distance distributions shown in Fig. 9 indicate that only about 2–3 cm of motion from the centroid can be expected, and the majority of the points are within 1 cm. These movement

TABLE I
SUMMARY DATA AND STATISTICS

Data	Two-Finger Condition	Three-Finger Condition	Figure
Object workspace centroid[1]	(−1.6 ± 0.4, −7.3 ± 0.4, 7.6 ± 0.3) cm	(−1.0 ± 0.4, −7.0 ± 0.4, 8.0 ± 0.3) cm	7
Object workspace PCA vector 1	(−0.2, 1.1, 1.7) cm	(−0.8, 1.1, 1.2) cm	7
Object workspace PCA vector 2	(0.8, 0.5, 0.6) cm	(0.7, 0.4, 0.6) cm	7
Object workspace PCA vector 3	(−0.1, −0.4, 0.3) cm	(−0.08, −0.34, 0.33) cm	7
Object workspace PCA vector 1 68% cone angle[2]	44°	32°	7
Object workspace PCA vector 2 68% cone angle[2]	52°	40°	7
Object workspace PCA vector 3 68% cone angle[2]	22°	24°	7
Mean object to thumb vector[3]	(−1.4, 1.4, 1.2) cm	(−1.3, 1.4, 1.2) cm	11
Mean object to index finger vector[3]	(1.2, −2.0, −0.7) cm	(0.0, −2.5, −0.8) cm	11
Mean object to middle finger vector[3]	n/a	(1.8, −1.9, −0.2) cm	11
Mean object to thumb vector 68% cone angle[2]	13°	11°	11
Mean object to index finger vector 68% cone angle[2]	10°	8°	11
Mean object to middle finger vector 68% cone angle[2]	n/a	8°	11

Length units in cm are based on a 17.5 cm length hand. All three element values are given in (ulnar, proximal, palmar) coordinates relative to the base frame skin sensor one-third of the way from the continuation of the wrist flexion crease to the bump from the fourth metacarpal head, along the fourth metacarpal (see Fig. 3).
[1]95% confidence interval based on standard error of the mean for each individual coordinate.
[2]Semi-vertical angle of cone expanded from mean vector to minimum size which includes 68% of orientations. See Section III-F.
[3]Mean vector from object workspace centroid to the centroid of each of the finger workspaces, as in Fig. 11.

ranges give an upper bound for the amount of motion that can be expected before arm/wrist motion or regrasping of an object will be required to accomplish a given displacement. The principal axis lengths can be used to provide a more nuanced view of these motion ranges. These small motion ranges are important because motion purely within the hand could increase precision by allowing the wrist/arm to be braced or stabilized, for example. Small within-hand movements ought to also reduce overall energy consumption relative to larger wrist or arm movements. Thus, an understanding of these motion ranges could be useful for high precision applications, such as surgery with hand-held surgical devices, ranging from simple passive tools (e.g., scalpels) to complex active robots, whether hand-held or tele-operated [15]. These motion ranges can also provide a baseline comparison for clinical assessment of a patient's range of motion, or to evaluate rehabilitation progress based on amount of recovery of workspace along the different principal axes found.

B. Workspace Shape

In addition to workspace size, the results show the shape and orientation of the workspace. In particular, most participants show a characteristic thin long arc in the proximal-palmar plane. This arc is the longest observed axis for the manipulation motion of the majority of participants. This shape suggests that if an application demands a long within-hand motion, it may be advantageous to align that motion with this long arc, generally in the palmar direction but with a slant away from the palm. The thinness of the arc also indicates that motions toward the palm, roughly along the palmar axis, are either difficult or at least very unintuitive for most participants. Tools, such as hand-held medical devices, can be designed to take advantage of the longer arcs of motion or more flexible areas of the workspace. It is possible that this characteristic motion arc could be used for clinical assessment as well. Having a patient perform a simple precision manipulation motion along this arc and measuring the range of motion achieved could be predictive of overall manipulation ability, but more work would be needed to assess the exact effect of this motion range on overall performance, such as performance of other related daily tasks.

Understanding the centroid location for the workspace may be quite useful. For example, hand-held devices can be designed to be comfortably held at a position close to the center of the precision manipulation workspace, to give the user greater flexibility of motion from their starting position. If manipulation tasks are used to evaluate hand function, tasks which allow a patient to start from or rest their fingers close to this region may be more comfortable and also allow freer motions. While we anticipated the relaxed starting locations of the participants might correspond well to the center of the Cartesian workspace, in practice, we found the starting locations to be no closer than a random point from the trials. This suggests that if it is important to precisely determine the center of the Cartesian precision manipulation workspace, an active exploration method may be necessary, and simply picking a relaxed starting location in the fingertips will give about 1 cm of error on average. However, further experiments may be necessary to further validate these results, since the initial position of the participants was simply a comfortable self-selected position and not rigorously controlled to a greater degree.

C. Interparticipant Variability

While certain aspects of the overall workspace shape are consistent across many participants, there is still extensive variability. The participants could be broken up into three ranges based on the workspace volumes achieved. The lowest volume group of about two to three participants appears to simply make small movements around a central point, resulting in a fairly spherical workspace. Most participants lie in a middle range, where the arc in the proximal-palmar plane becomes apparent and other ranges of motion also increase. Finally, there are two participants with the highest volumes who were able to produce a thicker arc, apparently adding a motion toward the palm that

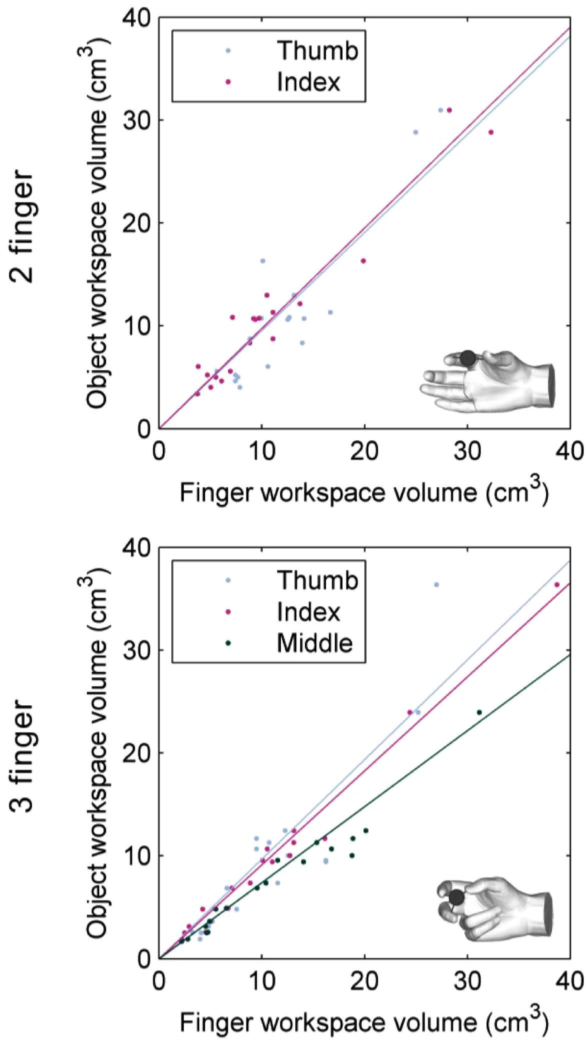

Fig. 12. Correlation between finger workspace volume and object workspace volume. The thumb and index finger volumes match closely to the object volume, while in the three-finger case, the middle finger traces out a larger volume than the object does.

most participants found difficult or at least highly unintuitive. We believe that the observed variability is likely a mix of motivation, what could be called motor creativity, as well as physical differences such as range of motion or finger pad characteristics. For example, a participant with a particularly sticky or compliant finger pad could enable secure manipulation through a wider range of motion.

D. Two- and Three-Finger Conditions and Finger Usage

In addition to intersubject variability, certain shifts are observed when the number of fingers used during the manipulation is changed. Overall, the two-fingered workspace is larger ($p < 0.001$), but this trend does not hold for every participant or trial. We expected a volume decrease due to the extra kinematic constraints from the additional finger, but the decrease may be less dramatic than expected due to the similar kinematics and compliance of the index and middle fingers, which can allow them to act as a unit together rather than further constraining the motion. However, the kinematics of the manipulation do shift, as evidenced in the tilt of the first principal axis toward the ulnar direction when adding the middle finger, as well as the individual fingertip use.

For the usage of the fingertips, it is noteworthy that the thumb and index finger workspaces do not simply align along the distal-proximal axis, but are tilted, moving distally, toward the ulnar direction. The thumb is also significantly further along the palmar axis relative to the other fingers in both the two- and three-finger cases.

The results showing the natural alignment of the thumb and fingers during precision manipulation can be used in various ways. For example, devices intended for precision manipulation, such as small tools, can be designed so that their outer shape matches up with the finger shapes comfortably when the fingers are in the positions observed. The motion ranges can be used to avoid having parts of a device unintentionally constrain hand motion. For rehabilitation, the typical positions of the thumb and fingers relative to the object can help to show which parts of the thumb and finger workspace might be most important to maintain or restore in order to enable effective precision manipulation.

E. Applications

As discussed above, this understanding of within-hand manipulation kinematics can be applied in various domains. For example, awareness of the within-hand manipulation ranges can help to effectively train precision tasks such as small scalpel cuts or soldering, by taking advantage of the largest motion ranges. Devices designed to take advantage of the within-hand motion ranges could enable better precision and potentially reduce fatigue, since wrist and arm movements would be reduced. When designing prosthetic or robotic hands, the angles of finger usage and ranges of motion common in precision manipulation could be imitated. A more precise understanding of precision manipulation workspace can also be used to help focus methods for rehabilitation or hand assessment. For example, since the workspace is quite small, using the longest motion axes for test motions could help to measure precision manipulation capability more accurately. These long motions may also be useful exercises during rehabilitation. In addition, the finger–object angles help show which parts of the finger workspace are most essential to maintain for successful precision manipulation, and where the fingers of the unimpaired hand are typically positioned.

VI. Limitations and Future Work

The present work can be extended in a number of ways. The current work analyzes the positional manipulation workspace and finger workspaces for only a single object. While efforts were made to select a comfortable object size which should allow a wide range of motions, different object sizes and shapes will impact the results. Objects that require different finger placement may have a particularly large effect, since the effective alignment of the kinematic constraints during manipulation would be altered. The present study also illustrates that training and motor creativity may have a significant effect on the resulting workspace. This suggests that different training methods could be tested to see if they can enhance the size of a participant's available manipulation workspace. Future work could also consider more complex manipulation tasks involving sliding at contact surfaces and adding/removing fingers during the task.

Despite the opportunities for further work, we believe the present work helps answer many basic questions about the precision manipulation workspace of the human hand, and that this basic information will be useful in a variety of domains, including biomechanics, rehabilitation, surgery, ergonomics, and device design.

REFERENCES

[1] M. R. Cutkosky, "On grasp choice, grasp models, and the design of hands for manufacturing tasks," *IEEE Trans. Robot. Autom.*, vol. 5, no. 3, pp. 269–279, Jun. 1989.

[2] G. Schlesinger, "Der mechanische Aufbau der kunstlichen Glieder," in *Ersatzglieder und Arbeitshilfen für Kriegsbeschädigte und Unfallverletzte*. Berlin, Germany: Springer, 1919, pp. 321–661.

[3] J. R. Napier, "The prehensile movements of the human hand," *J. Bone Joint Surg.*, vol. 38, no. 4, pp. 902–913, 1956.

[4] T. Feix *et al.*, "A comprehensive grasp taxonomy," in *Proc. Robot., Sci. Syst.: Workshop Understanding Human Hand Advancing Robot. Manipulation*, 2009.

[5] V. M. Zatsiorsky and M. L. Latash, "Multifinger prehension: An overview," *J. Mot. Behav.*, vol. 40, no. 5, pp. 446–76, Sep. 2008.

[6] I. M. Bullock *et al.*, "A hand-centric classification of human and robot dexterous manipulation," *IEEE Trans. Haptics*, vol. 6, no. 2, pp. 129–144, Apr.–Jun. 2013.

[7] I. Carpinella *et al.*, "Experimental protocol for the kinematic analysis of the hand: definition and repeatability," *Gait Posture*, vol. 23, no. 4, pp. 445–54, Jun. 2006.

[8] S. T. Leitkam *et al.*, "Determining functional finger capabilities of healthy adults: Comparing experimental data to a biomechanical model," *J. Biomech. Eng.*, vol. 136, no. 2, p. 021022, Feb. 2014.

[9] S. T. Leitkam and T. R. Bush, "Comparison between healthy and arthritic hand function using ranges of motion and a weighted fingertip space model," *J. Biomech. Eng.*, vol. 137, p. 041003, 2015.

[10] I. Carpinella *et al.*, "Multi-finger coordination in healthy subjects and stroke patients: a mathematical modelling approach," *J. Neuroeng. Rehabil.*, vol. 8, no. 1, p. 19, Jan. 2011.

[11] E. G. Cruz *et al.*, "Kinetic and kinematic workspaces of the index finger following stroke," *Brain*, vol. 128, no. Pt 5, pp. 1112–21, May 2005.

[12] G. Guthart and J. Salisbury, Jr., "The Intuitive telesurgery system: Overview and application," in *Proc. IEEE Int. Conf. Robot. Autom.*, 2000, pp. 618–621.

[13] T. H. Massie and J. K. Salisbury, "The PHANTOM haptic interface: A device for probing virtual objects," in *Proc. ASME Symp. Haptic Interfaces Virtual Environ. Teleoperator Syst.*, 1994, pp. 1–6.

[14] V. Datta *et al.*, "The use of electromagnetic motion tracking analysis to objectively measure open surgical skill in the laboratory-based model," *J. Am. Coll. Surg.*, vol. 193, no. 5, pp. 479–85, Nov. 2001.

[15] C. J. Payne and G.-Z. Yang, "Hand-held medical robots," *Ann. Biomed. Eng.*, vol. 42, no. 8, pp. 1594–605, Aug. 2014.

[16] M. A. Fehlberg *et al.*, "Active handrest: A large workspace tool for precision manipulation," *Int. J. Robot. Res.*, vol. 31, no. 3, pp. 289–301, Mar. 2012.

[17] R. Zheng and J. Li, "Kinematics and workspace analysis of an exoskeleton for thumb and index finger rehabilitation," in *Proc. IEEE Int. Conf. Robot. Biomimetics*, 2010, pp. 80–84.

[18] D. B. Slocum and D. R. Pratt, "Disability evaluation of the hand," *J. Bone Joint Surg.*, vol. 28, pp. 491–495, 1946.

[19] T. Feix *et al.*, "A metric for comparing the anthropomorphic motion capability of artificial hands," *IEEE Trans. Robot.*, vol. 28, no. 4, pp. 974–980, Aug. 2012.

[20] G. A. Kragten and J. L. Herder, "A platform for grasp performance assessment in compliant or underactuated hands," *J. Mech. Des.*, vol. 132, no. 2, p. 024502, 2010.

[21] L. Birglen and C. Gosselin, "Optimal design of 2-phalanx underactuated finger," in *Proc. Int. Conf. Intell. Manip. Grasping*, 2004, pp. 110–116.

[22] I. M. Bullock *et al.*, "Dexterous workspace of human two- and three-fingered precision manipulation," in *Proc. IEEE Haptics Symp.*, 2014, pp. 41–47.

[23] L.-C. Kuo *et al.*, "Functional workspace for precision manipulation between thumb and fingers in normal hands," *J. Electromyogr. Kinesiol.*, vol. 19, no. 5, pp. 829–839, Oct. 2009.

[24] C. Chang and Y. Sun, "Learning-based estimation of functional workspace in cooperative fingers motion," in *Proc. Int. Conf. Bioinformatics Biomed. Technol.*, 2012, vol. 29, pp. 141–145.

[25] Y. Youm and W. K. Chung, "Human kinematic factor for haptic manipulation: the wrist to thumb," in *Proc. 10th Symp. Haptic Interfaces Virtual Environ. Teleoperator Syst.*, 2002, pp. 319–326.

[26] R. Yokogawa and K. Hara, "Manipulabilities of the index finger and thumb in three tip-pinch postures," *J. Biomech. Eng.*, vol. 126, no. 2, pp. 212–219, 2004.

[27] J. Borras and A. M. Dollar, "A parallel robots framework to study precision grasping and dexterous manipulation," in *Proc. IEEE Int. Conf. Robot. Autom.*, 2013, pp. 3086–3092.

[28] L. U. Odhner and A. M. Dollar, "Dexterous manipulation with underactuated elastic hands," in *Proc. IEEE Int. Conf. Robot. Autom.*, 2011, pp. 5254–5260.

[29] R. R. Ma and A. M. Dollar, "Linkage-based analysis and optimization of an underactuated planar manipulator for in-hand manipulation," *J. Mech. Robot.*, vol. 6, pp. 011002-1–011002-9, 2013.

[30] L. Cui and J. S. Dai, "Posture, workspace, and manipulability of the metamorphic multifingered hand with an articulated palm," *J. Mech. Robot.*, vol. 3, no. 2, pp. 1–7, 2011.

[31] K. Rácz *et al.*, "An involuntary stereotypical grasp tendency pervades voluntary dynamic multifinger manipulation," *J. Neurophysiol.*, vol. 108, pp. 2896–2911, Sep. 2012.

[32] R. Gilster *et al.*, "Contact points during multidigit grasping of geometric objects," *Exp. Brain Res.*, vol. 217, no. 1, pp. 137–51, Mar. 2012.

[33] *Military Handbook: Anthropometry of US Military Personnel. (metric) DODHDBK 743A*, Feb. 1991.

[34] I. M. Bullock *et al.*, "Analyzing human fingertip usage in dexterous precision manipulation: Implications for robotic finger design," in *Proc. IEEE/RSJ Int. Conf. Intell. Robots Syst.*, 2014, pp. 1622–1628.

[35] N. I. Fisher *et al.*, *Statistical Analysis of Spherical Data*, 1st ed. Cambridge, U.K.: Cambridge Univ. Press, 1987.

Authors' photographs and biographies not available at the time of publication.